Preparation, Characterization and Facile Thermolysis of $[X_2GaP(SiMe_3)_2]_2$ (X = Br, I) and $(Cl_3Ga_2P)_n$: New Precursors to Nanocrystalline Gallium Phosphide

Steven R. Aubuchon, Andrew T. McPhail, and Richard L. Wells[*]

Department of Chemistry, Paul M. Gross Chemical Laboratory, Duke University, Durham, North Carolina 27708

Julia A. Giambra and James R. Bowser

Department of Chemistry, Houghton Hall, State University of New York—College at Fredonia, Fredonia, New York 14063

Received August 24, 1993. Revised Manuscript Received October 28, 1993[⊗]

$[Br_2GaP(SiMe_3)_2]_2$ and $[I_2GaP(SiMe_3)_2]_2$ have been prepared by the 1:1 mole ratio reaction of the corresponding gallium(III) halide with $(Me_3Si)_3P$. Direct introduction probe mass spectrometry indicates that the former product is dimeric in the gas phase; single-crystal X-ray analysis reveals that it is also dimeric in the solid state and it is isostructural with $[Cl_2GaP(SiMe_3)_2]_2$, but the crystals are not isomorphous. $[Br_2GaP(SiMe_3)_2]_2$ crystallizes in the orthorhombic system, space group *Pbca*, with $a = 13.803(2)$, $b = 16.652(2)$, $c = 13.636(2)$ Å, $V = 3134(1)$ Å^3, $D_{calc} = 1.725$ g cm^{-3} for $Z = 4$; the mean Ga–P bond length in the planar Ga–P–Ga–P core is 2.386 Å. Also described is the synthesis of $(Cl_3Ga_2P)_n$ via the 2:1 mole ratio reaction of $GaCl_3$ and $(Me_3Si)_3P$. All of the title compounds undergo thermolysis at relatively low temperature to yield nanocrystalline GaP. Thermolysis has been studied by thermal gravimetric analysis, and the resultant air-stable powders have been characterized by X-ray diffraction and elemental analysis.

Introduction

For the past decade, much of the research in the area of group 13–group 15 chemistry has been centered on the preparation of semiconductor precursors. Recently, the emphasis has shifted to the utilization of these precursors to form materials, in particular nanocrystalline or "quantum dot" semiconductors. These small particles are made up of clusters of molecules ranging in size from <1 to nearly 10 nm, which corresponds to agglomeration numbers of <10 up to a few hundred. The quantum confinement of electrons and holes in these low-dimensional structures strongly modifies the electronic properties of the semiconductor, which can greatly enhance various high-speed electron and optoelectronic devices.[1]

Previous research in our laboratory has demonstrated the utility of silylarsines for the preparation of compounds containing the gallium–arsenic bond. Thus, using reagents of the general formula $R_nAs(SiMe_3)_{3-n}$ and R'_nGaX_{3-n} (n = 0, 1, 2), a number of monomeric, dimeric and trimeric arsinogallanes have been synthesized.[2] Subsequent work has explored the more fundamental reactions in the series, namely, those between GaX_3 (X = Cl, Br) and $As(SiMe_3)_3$. We have shown that reactions involving these species in a 1:1 mole ratio proceed at relatively low temperatures to eliminate Me_3SiX with concomitant formation of GaAs.[3] Furthermore, the 2:1 mole ratio reaction of $GaCl_3$ and $(Me_3Si)_3As$ eliminates 3 mol equiv of Me_3SiCl to yield a yellow powder of empirical formula Cl_3Ga_2As (**1**) which has been shown to be an excellent precursor to nanocrystalline GaAs.[4]

Recent research has applied analogous reaction schemes to gallium–phosphorus systems, yielding both 1:1 adducts and a compound exhibiting mixed-bridging of two gallium centers by a phosphorus atom and a halogen.[5] Subsequent work centered on the preparation and characterization of a remarkably different compound, $[Cl_2GaP(SiMe_3)_2]_2$ (**2**). Through thermolysis, **2** undergoes labile dehalosilylation to yield a gallium phosphide-containing powder.[6]

Herein we report the extension of this research, including the preparation, characterization, and thermal decomposition of two analogs of **2**, viz. $[Br_2GaP(SiMe_3)_2]_2$ (**3**), and $[I_2GaP(SiMe_3)_2]_2$ (**4**). In common with **2**, compounds **3** and **4** undergo dehalosilylation upon heating to yield nanocrystalline GaP. This phenomenon has been examined by thermal gravimetric analysis (TGA), and the resultant GaP has been characterized by X-ray powder diffraction (XRD). In addition, we report the synthesis and subsequent thermal decomposition of $(Cl_3Ga_2P)_n$ (**5**), the phosphorus-containing analog of **1**. This light yellow powder eliminates $GaCl_3$ upon heating to yield nanocrystalline GaP.

Experimental Section

General Considerations. All manipulations were performed using general Schlenk, drybox, and/or high-vacuum techniques.

[⊗] Abstract published in *Advance ACS Abstracts*, December 1, 1993.

(1) Stucky, G. D. The Interface of Nanoscale Inclusion Chemistry. *Prog. Inorg. Chem.* **1992**, *40*, 99–178. Nötzel, R.; Ploog, K. H. *Adv. Mater.* **1993**, *5*, 22. Heinglein, A. *Chem. Rev.* **1989**, *89*, 1861.

(2) For a review, see: Wells, R. L. *Coord. Chem. Rev.* **1992**, *112*, 273.

(3) Wells, R. L.; Pitt, C. G.; McPhail, A. T.; Purdy, A. P.; Shafieezad, S.; Hallock, R. B. *Chem. Mater.* **1989**, *1*, 4.

(4) Wells, R. L.; Hallock, R. B.; McPhail, A. T.; Pitt, C. G.; Johansen, J. D. *Chem. Mater.* **1991**, *3*, 381.

(5) Wells, R. L.; Aubuchon, S. R.; Self, M. F.; Jasinski, J. P.; Woudenberg, R. C.; Butcher, R. J. *Organometallics* **1992**, *11*, 3370.

(6) Wells, R. L.; Self, M. F.; McPhail, A. T.; Aubuchon, S. R.; Woudenberg, R. C.; Jasinski, J. P. *Organometallics* **1993**, *12*, 2832.

0897-4756/94/2806-0082$04.50/0

Solvents (including those used for NMR spectra) were appropriately dried and distilled under argon prior to use. Literature methods were used to prepare $P(SiMe_3)_3$.[7] $GaBr_3$ was purchased from Alfa Products and purified by sublimation. GaI_3 was obtained from Roc-Ric, Inc. ^1H and $^{13}C\{^1H\}$ NMR spectra were obtained on a Varian XL-300 spectrometer at 300.0 and 75.4 MHz, respectively, and were referenced to TMS via the residual protons or carbons of C_7D_8. ^{31}P spectra were obtained on either a Varian XL-300 spectrometer at 121.4 MHz or a Varian Unity 500 spectrometer at 202.3 MHz and were referenced to external 80% H_3PO_4 at δ 0.00 ppm. Mass spectra were obtained on a Hewlett-Packard 5988A GC/MS/DS system. TGA data were obtained on a duPont Instruments Model 951 thermogravimetric analyzer. X-ray powder diffraction data were collected on a Phillips XRG 3000 diffractometer using Cu Kα radiation (λ = 1.5418 Å; graphite monochromator). Single-crystal X-ray diffraction data were recorded on an Enraf-Nonius CAD-4 diffractometer (Cu Kα radiation; graphite monochromator). Melting points (uncorrected) were taken in sealed capillaries (Thomas-Hoover Uni-melt). Elemental analysis was performed by E + R Microanalytical Laboratory, Inc., Corona, NY.

Preparation of $[Br_2GaP(SiMe_3)_2]_2$ (3). $GaBr_3$ (0.368 g, 1.20 mmol) in 150 mL of dry pentane was placed in a 250-mL round-bottom flask equipped with a Teflon screw cap and sidearm valve. $P(SiMe_3)_3$ (0.303 g, 1.21 mmol) dissolved in 50 mL of pentane was slowly added to the flask dropwise. The flask was capped and placed in a sonicating water bath for 16 h, after which the solvent and volatiles were removed in vacuo, affording a white solid. X-ray diffraction-quality crystals of **3** were grown from toluene in quantitative yield; mp decomposes above 220 °C. Anal. Calcd (found) for $C_6H_{18}Br_2GaPSi_2$: C, 17.71 (17.96); H, 4.46 (4.65); Br, 39.28 (39.00). ^1H NMR: δ 0.33 [d, 18H, Si*Me*$_3$ (monomer) (J_{P-H} = 5.99 Hz)], δ 0.49 [t, 36 H, Si*Me*$_3$ (dimer) (J_{P-H} = 3.33 Hz)]. $^{13}C\{^1H\}$ NMR: δ 1.9–2.1 [overlapping multiplet, PSi*Me*$_3$]. $^{31}P\{^1H\}$ NMR: δ −176.1 (s).

Preparation of $[I_2GaP(SiMe_3)_2]_2$ (4). GaI_3 (0.545 g, 1.21 mmol) in 100 mL of dry pentane was placed in a 250-mL round-bottom flask equipped with a Teflon screw cap and sidearm valve. $P(SiMe_3)_3$ (0.305 g, 1.22 mmol) dissolved in 15 mL of pentane was slowly added to the flask dropwise. The flask was capped and placed in a sonicating water bath for 14 h, after which the solvent and volatiles were removed in vacuo, affording a white solid that was collected in quantitative yield; mp decomposes above 220 °C. Anal. Calcd (found) for $C_6H_{18}GaI_2PSi_2$: C, 14.39 (14.29); H, 3.62 (3.67); I, 50.67 (50.95). ^1H NMR: δ 0.33 [d, 18H, Si*Me*$_3$ (monomer) (J_{P-H} = 5.75 Hz)], δ 0.53 [t, 36 H, Si*Me*$_3$ (dimer) (J_{P-H} = 3.18 Hz)]. $^{13}C\{^1H\}$ NMR: δ 2.28 [d, Si*Me*$_3$ (monomer) (J_{P-C} = 12.7 Hz)], δ 3.19 [t, Si*Me*$_3$ (dimer) (J_{P-C} = 4.1 Hz)]. $^{31}P\{^1H\}$ NMR: δ −209.7 (s).

Preparation of $(Cl_3Ga_2P)_n$ (5). $GaCl_3$ (0.535 g, 3.07 mmol) was dissolved in ca. 100 mL of pentane in a 250-mL round-bottom flask equipped with Teflon screw cap and sidearm valve. Dropwise addition of $(Me_3Si)_3P$ (0.372 g, 1.50 mmol) dissolved in ca. 5 mL of pentane led to the immediate formation of a white precipitate. The flask was capped and placed in a sonicating water bath for 15 h, resulting in a light yellow, insoluble powder. The solvent and volatiles were removed in vacuo. Titration of the hydrolyzed volatiles with NaOH (0.1007 N, 46.10 mL) corresponded to elimination of 4.49 mmol (99%) of Me_3SiCl. The resultant solid was washed in hot pentane, allowed to air dry, and collected in a 0.415-g (quantitative) yield.

Thermal Decomposition of $[Br_2GaP(SiMe_3)_2]_2$ (3) and $[I_2GaP(SiMe_3)_2]_2$ (4). Compounds **3** and **4** were decomposed independently, but in a similar manner. Samples of each compound [0.450 g (0.553 mmol) of **3**, 0.946 g (0.944 mmol) of **4**] were placed in a water-cooled sublimator with an attached Teflon valve. Under vacuum, the sublimator, in a sand bath and opened to a trap cooled to −196 °C, was slowly warmed over 3 h to 320 °C, at which it was maintained overnight. The resulting powder was then annealed for 1 h with a cool flame (400–500 °C). Over the course of the decomposition, the color of the initially white material changed to yellow then orange, and eventually to a brown powder [0.0615 g (55.4% yield) and 0.147 g (77.4% yield) from **3** and **4**, respectively]. Volatiles collected from the decomposition of **3** were hydrolyzed with deionized water; titration with NaOH (0.109 N, 18.60 mL) indicated the elimination of 2.03 mmol (91.8%) of Me_3SiCl. The brown powders were washed with hot toluene, then hot pentane, allowed to air-dry, and analyzed by XRD and partial elemental analysis. Anal. Calcd (found) for GaP: Decomposition of **3**: Ga, 69.24 (56.07); P, 29.36 (30.76); C, 0.00 (3.23); H, 0.00 (0.37) (P:Ga mol ratio = 1.18). Decomposition of **4**: Ga, 69.24 (54.00); P, 30.76 (30.48); C, 0.00 (2.71); H, 0.00 (0.30); I, 0.00 (7.65) (P:Ga mol ratio = 1.27).

Table 1. Crystallographic Data for $[Br_2GaP(SiMe_3)_2]_2$ (3)

molecular formula	$C_{12}H_{36}Br_4Ga_2P_2Si_4$
formula weight	813.79
crystal system	orthorhombic
space group	*Pbca*(D_{2h}^{15}) (No. 61)
a (Å)	13.803(2)
b (Å)	16.652(2)
c (Å)	13.636(2)
V (Å^3)	3134(1)
Z	4
D_{calcd} (g cm^{-3})	1.725
μ(Cu Kα radiation, λ = 1.5418 Å)	106.5
temp (°C)	23
crystal dimensions (mm)	0.36 × 0.36 × 0.40
$T_{max}:T_{min}$	1.00:0.57
scan type	$\omega-2\theta$
scan width (deg)	$0.80 + 0.14 \tan\theta$
θ_{max} (deg)	75
intensity control refls variation; repeat time (h)	331, 312, 233, 234; −20%; 2
total no. of nonequiv reflns ($+h,+k,+l$) recorded	3208
no. of reflns retained [$I > 3.0\sigma(I)$]	1736
no. of parameters refined	110
extinction correction	3.3(3) × 10^{-7}
$R(R_w)$[a]	0.043(0.058)
goodness-of-fit[b]	1.45
max shift: esd in final least-squares cycle	0.01
final $\Delta\rho$ (e/Å^3) max; min	0.70; −0.63

[a] $R = \sum||F_o| - |F_c||/\sum|F_o|$; $R_w = [\sum w(|F_o| - |F_c|)^2/\sum w|F_o|^2]^{1/2}$; $\sum w\Delta^2[w = 1/\sigma^2(|F_o|), \Delta = (|F_o| - |F_c|)]$ was minimized. [b] Goodness-of-fit = $[\sum w\Delta^2/(N_{observations} - N_{parameters})]^{1/2}$.

Thermal Decomposition of $(Cl_3Ga_2P)_n$ (5). A 0.410-g (1.48 mmol) sample of **5** was placed in a water-cooled sublimator and opened to vacuum. The temperature was raised to 300 °C over 2 h during which time the material changed to a dark brown color, and a yellowish-white crystalline material collected on the coldfinger. The temperature was then raised to 440 °C for 2 h. The resulting dark brown material was washed with ca. 25 mL of hot toluene and allowed to air dry, after which it was collected in a 0.138-g (92.6%) yield. Anal. Calcd (found) for GaP: Ga, 69.24 (60.90, 60.65); P, 30.76 (30.80, 29.92); Cl, 0.0 (1.86, 1.70) (P:Ga mol ratio = 1.14, 1.10).

Structural Analysis of 3. Crystallographic data and data collection parameters are summarized in Table 1. Refined unit-cell parameters were derived from the diffractometer setting angles for 25 reflections (36° < θ < 40°) widely separated in reciprocal space. The intensities of four reference reflections, remeasured every 2 h during data collection, showed significant loss (20%) indicating crystal deterioration. Intensity data were corrected for the usual Lorentz and polarization effects; linear decay and empirical absorption corrections were also applied. The space group *Pbca* was established uniquely by the Laue symmetry in combination with the systematic absences: $0kl$ when $k \neq 2n$, $h0l$ when $l \neq 2n$, $hk0$ when $h \neq 2n$. With four formula units in the unit cell, the dimeric molecules are required to lie on crystallographic centers of symmetry. The crystal structure was solved by direct methods (MULTAN11/82). Approximate coordinates for the gallium, bromine, phosphorus, and silicon atoms were derived from an E map; carbon atoms were located in a weighted F_o Fourier synthesis phased by these heavier atoms. Atomic positional and thermal parameters (at first isotropic, then anisotropic) were adjusted by means of full-matrix least-squares

---

(7) Becker, G.; Schmidt, H.; Uhl, G.; Uhl, W. *Inorg. Synth.* **1990**, *27*, 243.

(8) Cromer, D. T.; Waber, J. T. *International Tables for X-ray Crystallography*; The Kynoch Press: Birmingham, England, 1974; Vol IV.

Table 2. Non-Hydrogen Atom Fractional Coordinates and Equivalent Isotropic Thermal Parameters for 3, with Estimated Standard Deviations in Parentheses

atom	x	y	z	B_{eq} (Å^2)
Ga	0.03711(6)	0.05261(5)	0.09482(6)	2.93(1)
P	−0.0870(1)	0.0720(1)	−0.0245(1)	2.92(3)
Br(1)	−0.01582(8)	0.04978(6)	0.25613(6)	5.38(2)
Br(2)	0.15778(7)	0.15003(6)	0.09042(8)	5.65(2)
Si(1)	−0.2411(2)	0.0676(1)	0.0385(2)	3.97(4)
Si(2)	−0.0627(2)	0.1849(1)	−0.1166(2)	4.41(5)
C(1)	−0.2514(8)	−0.0167(6)	0.1221(7)	6.1(2)
C(2)	−0.3267(8)	0.0568(9)	−0.0643(9)	9.1(4)
C(3)	−0.2630(9)	0.1629(6)	0.1044(8)	6.8(3)
C(4)	−0.1632(10)	0.1915(6)	−0.2069(8)	7.7(3)
C(5)	−0.0622(10)	0.2727(5)	−0.0308(8)	6.6(3)
C(6)	0.0573(9)	0.1751(6)	−0.1798(7)	6.3(2)

iterations. In the later cycles, hydrogen atoms were incorporated at their calculated positions (C–H = 1.05 Å) and an extinction correction was included as a variable. A final difference Fourier synthesis contained no unusual features. Non-hydrogen atom fractional coordinates and equivalent isotropic thermal parameters are listed in Table 2.

Crystallographic calculations were performed on PDP11/44 and MicroVAX computers by use of Enraf-Nonius structure determination package (SDP). For all structure factor calculations, neutral atom scattering factors and their anomalous dispersion corrections were taken from ref 8.

Results and Discussion

Previous research in our laboratory has proven the utility of dehalosilylation to form precursors to GaAs. In 1990, Alivisatos et al.[9] reported that GaAs nanocrystals are produced by a specific dehalosilylation reaction (eq 1)as

$$GaCl_3 + (Me_3Si)_3As \rightarrow GaAs + 3Me_3SiCl \qquad (1)$$

initially carried out in our laboratories.[3] Furthermore, in some important experiments, they demonstrated that the same reaction carried out in quinoline afforded somewhat smaller crystallites that are soluble in pyridine as well as quinoline.[8] Subsequent work examined the 2:1 mole ratio reaction of $GaCl_3$ and $(Me_3Si)_3As$. The product of this reaction is the yellow powder $(Cl_3Ga_2As)_n$ (**1**).[4] Upon heating, **1** eliminates $GaCl_3$ via a novel reaction pathway to give microcrystalline GaAs.

Uchida et al.[10] have investigated similar reactions in the In–As system. They report the synthesis of indium arsenide nanocrystals from the reaction of indium(III) acetylacetonate [In(acac)$_3$] and $(Me_3Si)_3As$ in triglyme. The resultant brown colloids were shown to contain InAs crystallites ranging from 1 to 8 nm in diameter but the nature of the byproducts were not reported. Although both Steigerwald and co-workers[11] and Theopold and co-workers[12] have applied similar reaction pathways to produce InP, only the latter have reported materials approaching the nanocrystalline range.

Recently, we reported the synthesis, characterization, and subsequent thermolysis of $[Cl_2GaP(SiMe_3)_2]_2$ (**2**), a new precursor to GaP.[6] Compound **2** results from the 1:1 mole ratio reaction of $GaCl_3$ and $(Me_3Si)_3P$ (eq 2)and is the first structurally characterized example of a Ga–P

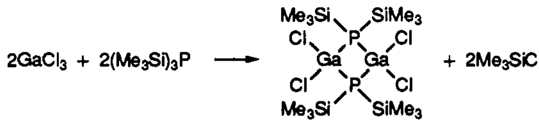

(2)

dimer containing all exocyclic halogen ligands on the metal center. In addition, **2** has been thermally decomposed to eliminate Me_3SiCl and yield GaP with a small amount of impurities. As an extension of this work, we have investigated the reactions of $GaBr_3$ and GaI_3 with $(Me_3Si)_3P$ in both 1:1 and 2:1 mole ratios, as well as the 2:1 mole ratio reaction of $GaCl_3$ and $(Me_3Si)_3P$.

The reaction of $GaBr_3$ with $(Me_3Si)_3P$ in a 1:1 mole ratio yields $[Br_2GaP(SiMe_3)_2]_2$ (**3**) with concomitant formation of Me_3SiBr. Like that of its chloro analog **2**, the solution ^1H NMR spectrum of **3** exhibits a doublet and a triplet in the methyl region, attesting to the presence of both monomeric and dimeric species in solution. Direct introduction probe mass spectrometry shows a parent ion at $m/z = 813$, which confirms the dimeric nature of **3** in the gas phase. The solid-state structure is in accord with NMR and mass spectral data. Compound **3** crystallizes with four discrete dimers lying on crystallographic centers of symmetry in the unit cell of orthorhombic space group *Pbca*. Although **3** is isostructural with **2**, crystals of these compounds are not isomorphous. An ORTEP diagram showing the crystallographic atom numbering scheme and solid-state conformation of **3** is presented in Figure 1. Bond lengths and angles are provided in Table 3. The Ga–P–Ga–P ring is strictly planar, and it is distorted from square in the same manner as that in **2** [P–Ga–P′ = 92.92(6)° > Ga–P–Ga′ = 87.08(6)°]. Bonding geometries at P and Ga are distorted tetrahedral with Si(1)–P–Si(2) = 111.6(1)° and Br(1)–Ga–Br(2) = 105.33(5)°. The mean of the Ga–P bond distances [2.385(2), 2.387(2) Å] at 2.386 Å is slightly longer than that of 2.379 Å in **2**,[6] reflecting the decreased acidity of the gallium centers as well as the greater steric demands of bromine versus chlorine. The mean Ga–Br bonded distance at 2.322 Å lies close to the corresponding means of 2.331 Å in $[GaBr_2(tetrahydrofuran)]_3As$[13] and 2.329 Å in $[(Me_3SiCH_2)_2AsGaBr_2]_3$,[14] but it is significantly shorter than the 2.378(1) Å length in the much more sterically crowded $\{[(Me_3SiCH_2)_2As]_2GaBr\}_2$.[15] P–Si bonded distances average 2.291 Å, similar to their mean of 2.287 Å in **2**.

The 1:1 mole ratio reaction of GaI_3 with $(Me_3Si)_3P$ produces $[I_2GaP(SiMe_3)_2]_2$ (**4**), which is the analog not only of **2** and **3** in the Ga–P system but also of a compound previously reported in the Ga–As system, $[I_2GaAs(SiMe_3)_2]_2$ (**6**).[16] It is interesting that to date **6** is the only fully characterized compound in the Ga–As system with all exocyclic halogen ligands on the gallium centers. Whereas the reactions between lighter gallium(III) halides with $(Me_3Si)_3As$ proceed completely to form GaAs,[3] the analogous reactions in the Ga–P system eliminate only one molar equivalent of silyl halide to yield dimeric species.

Compound **4** exhibits dual resonances in the methyl region of the solution ^1H NMR spectrum, indicating the

---

(9) Olshavsky, M. A.; Goldstein, A. N.; Alivisatos, A. P. *J. Am. Chem. Soc.* **1990**, *112*, 9438.

(10) Uchida, H.; Matsunga, T.; Yoneyama, H.; Sakata, T.; Mori, H.; Sasaki, T. *Chem. Mater.* **1993**, *5*, 716.

(11) Stuczynski, S. M.; Opila, R. L.; Marsh, P.; Brennan, J. G.; Steigerwald, M. L. *Chem. Mater.* **1991**, *3*, 379.

(12) Douglas, T.; Theopold, K. H. *Inorg. Chem.* **1991**, *30*, 596.

(13) Wells, R. L.; Shafieezad, S.; McPhail, A. T.; Pitt, C. G. *J. Chem. Soc., Chem. Commun.* **1987**, 1823.

(14) Wells, R. L.; Purdy, A. P.; McPhail, A. T.; Pitt, C. G. *J. Organomet. Chem.* **1988**, *354*, 287.

(15) Purdy, A. P.; Wells, R. L.; McPhail, A. T.; Pitt, C. G. *Organometallics* **1987**, *6*, 2099.

(16) Johansen, J. D.; McPhail, A. T.; Wells, R. L. *Adv. Mater. Opt. Electron.* **1992**, *1*, 29.

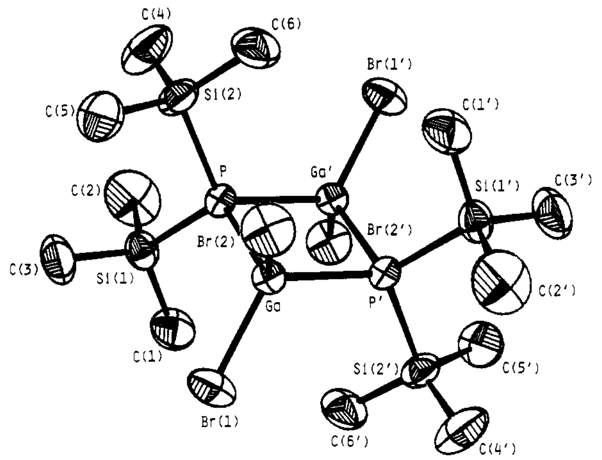

Figure 1. ORTEP diagram (50% probability ellipsoids) showing the crystallographic atom numbering scheme and solid-state conformation of $[Br_2GaP(SiMe_3)_2]_2$ (**3**).

Table 3. Interatomic Distances (Å) and Angles (deg) for 3,[a] with Estimated Standard Deviations in Parentheses[a]

	(a) Bond Lengths		
Ga–P	2.385(2)	Si(1)–C(1)	1.81(1)
Ga–P′	2.387(2)	Si(1)–C(2)	1.84(1)
Ga–Br(1)	2.318(1)	Si(1)–C(3)	1.85(1)
Ga–Br(2)	2.326(1)	Si(2)–C(4)	1.86(1)
P–Si(1)	2.295(3)	Si(2)–C(5)	1.87(1)
P–Si(2)	2.286(3)	Si(2)–C(6)	1.87(1)
	(b) Bond Angles		
P–Ga–P′	92.92(6)	P–Si(1)–C(1)	109.4(4)
P–Ga–Br(1)	115.07(5)	P–Si(1)–C(2)	108.2(4)
P–Ga–Br(2)	113.73(6)	P–Si(1)–C(3)	107.8(4)
P′–Ga–Br(1)	117.02(5)	C(1)–Si(1)–C(2)	110.6(6)
P′–Ga–Br(2)	112.91(5)	C(1)–Si(1)–C(3)	110.2(5)
Br(1)–Ga–Br(2)	105.33(5)	C(2)–Si(1)–C(3)	110.4(6)
Ga–P–Ga′	87.08(6)	P–Si(2)–C(4)	107.7(4)
Ga–P–Si(1)	114.0(1)	P–Si(2)–C(5)	107.4(3)
Ga–P–Si(2)	112.4(1)	P–Si(2)–C(6)	108.1(4)
Ga′–P–Si(1)	113.0(1)	C(4)–Si(2)–C(5)	111.8(5)
Ga′–P–Si(2)	116.9(1)	C(4)–Si(2)–C(6)	111.1(5)
Si(1)–P–Si(2)	111.6(1)	C(5)–Si(2)–C(6)	110.6(6)

[a] Primed atoms are related to the unprimed atoms by a crystallographic center of symmetry.

expected monomer–dimer equilibrium. Peak integration indicates that the doublet (monomer peak) is much larger than the triplet (dimer) in the case of **4** than it is for **2** and **3**, suggesting that the iodine-containing monomer is more stable than the bromo or chloro analogs, which is in accordance with the relative steric bulk of the iodine ligand. The volatility of **4** is also less than that of **2** or **3**, as evidenced by the inability to obtain a mass spectrum of the compound.

The reaction of $GaCl_3$ and $(Me_3Si)_3P$ in a 2:1 mole ratio eliminates 3 mol equiv of Me_3SiCl to yield an off-white powder of empirical formula Cl_3Ga_2P (**5**) in quantitative yield. This insoluble powder is the phosphorus containing analog of **1**. It is noteworthy that the analogous 2:1 mole ratio reactions of $GaBr_3$ or GaI_3 with $(Me_3Si)_3P$ result in very unstable yellow powders, which readily decompose to oils upon standing under an inert atmosphere.

It is well established that dehalosilylation is a viable reaction pathway for the formation of precursors to group 13–15 semiconductors. The presence of both halogen and $SiMe_3$ groups in **2–4** provided excellent opportunities to investigate the utility of further intramolecular dehalosilylation through thermolysis as a means to synthesize materials. Each of the compounds was independently thermally decomposed under vacuum, and the collected volatiles were analyzed. Upon heating, compounds **3–5** exhibit color changes, starting as white crystalline materials, going through shades of yellow and orange, and finally annealing as dark brown powders. Compound **2** was decomposed in a similar manner, but was not flame annealed. The (111), (220), and (311) zinc blende peaks of GaP are clearly evident in the XRD patterns (see Figure 2) recorded from each of the resultant air-stable brown powders. The broadness of the peaks is indicative of nanocrystalline particles, confirmed by application of the Debye–Scherrer formula[17] which indicates an average domain size of ca. 3 nm for compounds **3–5**. When the material is not annealed, a smaller domain size of ca. 1 nm is produced, as evidenced by the XRD pattern for the decomposition product of compound **2**. Thus, the GaP domain size appears to be dependent on the duration and temperature of the annealing process.

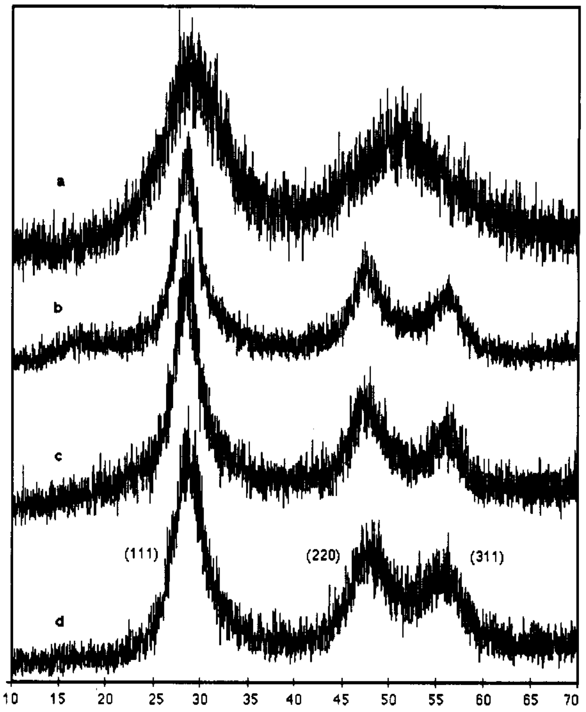

Figure 2. X-ray powder diffraction patterns of the materials resulting from the thermal decomposition of (a) $[Cl_2GaP(SiMe_3)_2]_2$ (**2**), (b) $[Br_2GaP(SiMe_3)_2]_2$ (**3**), (c) $[I_2GaP(SiMe_3)_2]_2$ (**4**), and (d) $(Cl_3Ga_2P)_n$ (**5**).

Titration of the hydrolyzed volatiles of the thermolysis confirmed the elimination of silyl halide. Elemental analyses of the brown powders indicate a relatively large amount of impurity, as well as an excess of phosphorus. As the reactor used was relatively low-tech, and the experimental conditions were not optimized, these results are not unexpected. This phenomenon has been seen previously by Kaner and co-workers in the solid-state synthesis of group 13–15 semiconductors.[18]

The thermolysis of **2–4** has also been studied by TGA. Samples were heated at a rate of 3 °C/min. under a stream of nitrogen. TGA data confirm that the dimeric compounds eliminate distinct molar equivalents of silyl halide

---

(17) Klug, H. P.; Alexander, L. E. *X-Ray Diffraction Procedures*; John Wiley & Sons: New York, 1954; Chapter 9.

(18) Treece, R. E.; Macala, G. S.; Rao, L.; Franke, D.; Eckert, H.; Kaner, R. B. *Inorg. Chem.* **1993**, *32*, 2745.

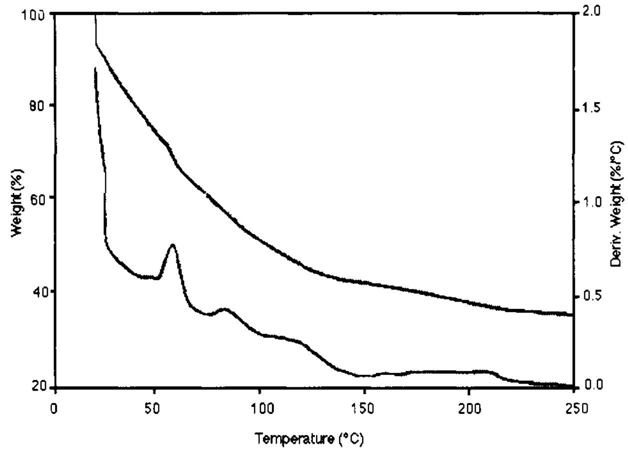

Figure 3. Thermal gravimetric analysis data for $[Cl_2GaP(SiMe_3)_2]_2$ (**2**).

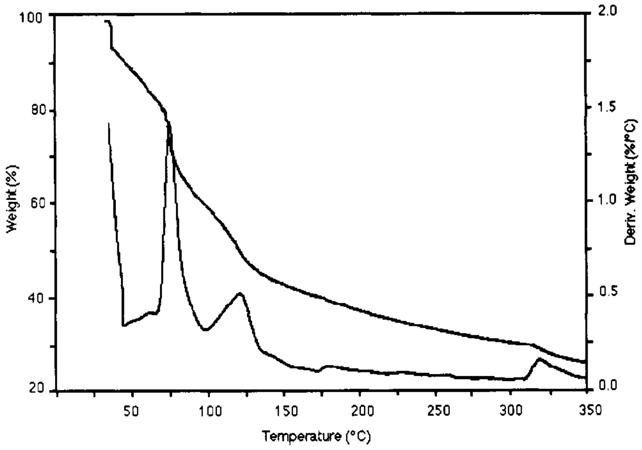

Figure 4. Thermal gravimetric analysis data for $[Br_2GaP(SiMe_3)_2]_2$ (**3**).

upon decomposition. In the case of $[Cl_2GaP(SiMe_3)_2]_2$ (**2**), there are two or perhaps three transitions, which cannot be individualized even at a very slow heating rate (Figure 3). Since the peak resolution is poor, sequential losses cannot be identified with reliability. Nevertheless, ca. 65% of the overall mass is eliminated at temperatures less than 250 °C, corresponding to the elimination of 2 mol equiv of Me_3SiCl per monomer unit. Thermolysis of $[Br_2GaP(SiMe_3)_2]_2$ (**3**) parallels that for **2**, with slightly better resolution in the TGA. Two sequential mass losses of ca. 37% correspond well to a stepwise elimination of Me_3SiBr. Total elimination of Me_3SiBr is complete below 350 °C (Figure 4). In the case of $[I_2GaP(SiMe_3)_2]_2$ (**4**), the TGA shows a distinct mass loss, centered roughly at 195 °C (see Figure 5). Although the thermogram of this compound is not as well resolved, the major peak (195 °C) corresponds to an average mass loss consistent with elimination of 1 mol equiv of Me_3SiI. In accord with expectations, the thermal stabilities of these dimeric species appear to increase as the atomic mass of the halide is increased.

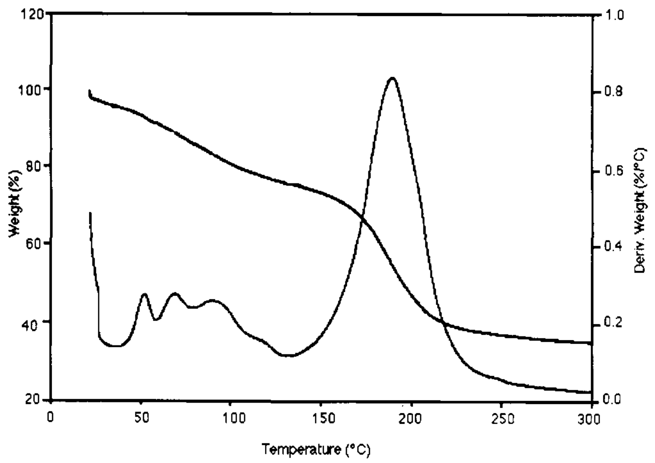

Figure 5. Thermal gravimetric analysis data for $[I_2GaP(SiMe_3)_2]_2$ (**4**).

In previous work, it was shown that $(Cl_3Ga_2As)_n$ (**1**), the arsenic analog of $(Cl_3Ga_2P)_n$ (**5**), eliminates $GaCl_3$ upon heating to produce microcrystalline GaAs.[4] Thermolysis of **5** was therefore undertaken to determine if it would decompose in a similar manner to furnish GaP. Upon heating the initially off-white solid to 200 °C, it began to turn yellow. Further heating to 300 °C resulted in a dark brown powder, with a yellowish-white crystalline sublimate. XRD of the brown powder confirmed the presence of GaP (see Figure 2). The thermolysis of **5** was also investigated by TGA, but it resulted in somewhat indecipherable data due to the different experimental conditions. Thus, bench-top decomposition of $(Cl_3Ga_2P)_n$ was performed under vacuum, facilitating the sublimation of $GaCl_3$ from the material, whereas TGA was carried out under a stream of nitrogen gas, possibly hindering the decomposition pathway. Moreover, in all the TGA experiments, decomposition temperatures fluctuated as a function of nitrogen flow rate.

Until recently, the preparation of group 13–15 semiconductor materials has been an arduous task, usually involving toxic and dangerous precursor materials. The synthesis and subsequent thermal decomposition of the title compounds should provide an alternative, facile route to nanocrystalline gallium phosphide. Future work will address applications into alternative 13–15 systems, including investigation of precursors for ternary and quaternary materials.

Acknowledgment. This work was generously supported by the Air Force Office of Scientific Research, The Office of Naval Research, and The Lord Foundation of North Carolina. J.R.B. acknowledges the financial support of TA Instruments, Inc.

Supplementary Material Available: Tables of hydrogen atom coordinates and isotropic thermal parameters, anisotropic temperature factors, and torsion angles for **3** (4 pages); table of observed and calculated structure amplitudes for **3** (12 pages). Ordering information is given on any current masthead page.